# Technical note: Flow cytometry assays for the detection, counting and cell-sorting of polyphosphate-accumulating bacteria

Clémentin Bouquet[1], Hermine Billard[1,2], Cécile C. Bidaud[3], Jonathan Colombet[1,2], Young-Tae Chang[4], Karim Benzerara[3], Fériel Skouri-Panet[3], Elodie Duprat[3], Anne-Catherine Lehours[1]

[1]Université Clermont Auvergne, CNRS, LMGE, F-63000 Clermont-Ferrand, France
[2]UCA Partner, Cytometry, Sort and Transmission Electronic Microscopy (CYSTEM) platform, F-63000 Clermont-Ferrand, France
[3]Sorbonne Université, Muséum National d'Histoire Naturelle, UMR CNRS 7590 – Institut de Minéralogie, de Physique des Matériaux et de Cosmochimie (IMPMC), Paris, France
[4]Department of Chemistry, Pohang University of Science and Technology (POSTECH), Pohang 37673, Republic of Korea

Correspondence to: Anne-Catherine Lehours (a-catherine.lehours@uca.fr)

**Abstract.** In the context of the ecological sustainability of phosphorus, the emerging evidence of the ubiquitous presence of polyphosphate-accumulating bacteria in natural environments invites efforts to reveal their unknown functions and roles in the biogeochemical cycle of phosphorus. This requires high-throughput methods to characterise the structure and dynamics of polyphosphate-accumulating bacteria in the environment. A promising strategy is to combine efficient staining of intracellular polyphosphate granules and their subsequent detection by flow cytometry, enabling rapid data acquisition and multiparametric analysis. In this study, we provide a generic protocol and we point out the potential pitfalls and limitations of the detection and quantification of polyphosphate-accumulating bacteria by flow cytometry using the dye 4'6-diamidino-2-phenylindole (DAPI). The assays were performed using *Tetrasphaera elongata*, a Gram-positive bacterium well known to accumulate large amounts of intracellular polyphosphates. A Gram-negative bacterial strain characterised by very low quantities of cellular polyphosphate was also included in analyses and tests were carried out on water and lake sediment samples. We also show that the synthetic fluorochrome JC-D7, a new selective fluorescent dye used for the specific labeling of endogenous polyphosphate in living cells, is promising for achieving these purposes, particularly in complex environmental samples.

## 1 Introduction

Since the "green revolution" of the 1960s, the phosphorus (P) contained in geological deposits has been extracted in large quantities for the production of fertilisers, increasing the input of P to the biosphere fourfold compared with the pre-industrial era (Falkowski *et al.*, 2000). Over the same period, P storage in terrestrial and freshwater ecosystems increased dramatically (> 75 %, Bennett *et al.*, 2001). This excess P has led to a deterioration in ecosystem services, notably the formation of hundreds of coastal dead zones associated with eutrophication (Diaz and Rosenberg, 2008). Paradoxically, and by analogy with "peak oil", a "phosphorus peak" is predicted by 2035 (Cordell *et al.*, 2009; 2011). To ensure the ecological sustainability of P, holistic approaches that combine microbiology, ecology, and geochemistry are needed. In this vein, there is emerging evidence of the unexpected and ubiquitous presence of polyphosphate-accumulating bacteria (PAB) in natural environments such as rivers, lakes, and soils, inviting efforts to reveal their unknown functions and roles in the context of P availability and cycling (Rivas-Lamelo *et al.*, 2017; Akbari *et al.*, 2021; Bidaud *et al.*, 2022).

Intracellular polyphosphates (polyP) are polymers containing from a few to hundreds orthophosphate residues linked together by phosphoanhydride bonds. Monovalent or divalent metal elements, such as $Mg^{2+}$, $K^{+}$, $Ca^{2+}$ and $Na^{+}$ can act as counterions in polyP polymers, forming complexes with the negatively charged phosphate residues (Akbari *et al.,* 2021). PolyP occurs as a ubiquitous biopolymer in representatives of all kingdoms of living organisms and every cell type in nature (Lorenzo-Orts *et al.* 2020, Akbari *et al.* 2021). Likely a key agent in evolution from prebiotic time (Brown and Kornberg, 2004; Lorentzo-Orts *et al.,* 2020), the functional roles of polyP in the cells of contemporary organisms are many and varied (Konberg *et al.,* 1999). PolyP can serve as a source of energy; as a phosphorylating agent for alcohols, including sugars, nucleosides, and proteins; and as a means of activating the precursors of fatty acids, phospholipids, polypeptides, and nucleic acids (Rao *et al.,* 2009). In PAB, the storage of polyP is exacerbated and polyP granules, which are spherical aggregates, can account for up to 20 % of the dry weight of these bacteria. PAB cells accumulate these polymers at cellular concentrations up to millimolar, for example, as an energy reserve to adapt and survive environmental gradients or to scavenge nutrients (Martin *et al.,* 2014). PolyP accumulation in PAB can have an impact on P biogeochemistry, and PAB are expected to play critical roles as reservoirs or catalysts for P exchange between the geosphere and the biosphere (Diaz *et al*., 2008; Cosmidis *et al*., 2014); yet they are still missing from the global P cycle models.

Numerous methodologies to quantify and characterise polyP have been developed, including chemical, biological, molecular and microscopic approaches (Majed *et al.* 2012). Most conventional analytical methods (*e.g*. electron ionisation mass spectrometry) require extensive sample preparation, pre-treatment and pre-fractionation procedures. Advanced analytical techniques, such as nuclear magnetic resonance, Raman, Raman-FISH (Fernando *et al*. 2019) and X-ray spectromicroscopy require much less pre-treatment and allow polyP to be characterised with high molecular and spatial resolution (< to µm). While the potential of these approaches in environmental and biological research is clear, their use remains limited due to the cost and accessibility of analysis instruments. Photometric approaches offer an interesting alternative to the methods discussed above and, the most relevant to date, are based on the interaction between polyP and the fluorochrome 4', 6-diamidino-2-phenylindole (DAPI) (Martin and Van Mooy, 2013). The binding of polyP to DAPI shifts the wavelength of maximum emission from DAPI and, as a result, the intensity of fluorescence intensity at this shifted wavelength is proportional to the concentration of intracellular polyP concentration. This principle has played a decisive role in visual identification of polyP granules in cells. These approaches which combine microscopic observations with DAPI labeling are simple but time-consuming techniques. Unveiling the environmental significance of PAB and their effects on biogeochemical P cycle requires high-throughput methods to characterise their structure, dynamics, and function in complex and heterogeneous environmental samples (Günther *et al*. 2009). To this end, a promising strategy is to combine the specific staining of intracellular polyP granules in PAB and their subsequent detection by flow cytometry (*e.g*., Zilles *et al.,* 2002; Günther *et al*., 2009; Terashima *et al.,* 2020).

Flow cytometry (FCM) is an essential tool in the field of environmental microbiology, enabling rapid data acquisition and multiparametric analyses. In combination with various dyes, FCM can be used to study communities and analyse thousands of microbial cells per second. The ability of fluorescence-activated cell sorting (FACS) also makes FCM a powerful technique for identifying and isolating microbial cells with particular characteristics (Zilles *et al*., 2002; Terashima *et al.,* 2020). Although FCM has already been applied to detect polyP fluorescence induced by different dyes (Zilles *et al*., 2002; Terashima *et al.,* 2020), there is still a lack of knowledge about optimal FCM parameters for the detection and counting of PAB from the environment.

In order to optimise detection and enumeration of PAB by FCM, we present here a detailed evaluation of a wide range of factors likely to affect the quality of the fluorescent signal and therefore the efficiency of enumeration from DAPI staining of polyP. We also compare DAPI staining with that obtained with JC-D7, which is a benzimidazolinium dye. Although this novel polyP sensor has been shown to be suitable for staining polyP in living eukaryotic cells and tissues (Angelova *et al.*, 2014), it has not yet been used to target PAB. The assays were performed using *Tetrasphaera elongata*, which represent up to 30 % of the total bacteria in enhanced biological phosphorus removal process (Nguyen *et al*., 2011). We also included in our analyses, a bacterial strain characterised by very low quantities of cellular polyP and carried out tests on water and lake sediment samples. Our work provides a generic protocol and highlights the potential pitfalls and limitations of PAB detection and quantification by FCM. It also pointed out that the JC-D7 dye is a promising fluorescent probe for achieving these purposes, particularly for the enumeration of PAB in environmental samples.

## 2 Material and methods

### 2.1. Strains and culture conditions

*Tetrasphaera elongata* Lp2 (DSM 14184), a gram-positive bacterium well known to accumulate large amounts of intracellular polyP (up to 30-35 % of the total biovolume of bacteria, Nguyen *et al.* 2011), was used as a "high polyP accumulator" control. Cells were grown in NM-1 medium (pH 7.1) containing (per litre): glucose (0.5 g); peptone (0.5 g); monosodium glutamate (0.5 g); yeast extract (0.5 g); $K_2HPO_4$ (0.44 g); $(NH_4)_2SO_4$ (0.1 g); $MgSO_4$ x $7H_2O$ (0.1 g). As there is no true negative control, prior to this study we screened our library of bacterial strains at the Laboratoire Microorganismes: Génome et Environnement (LMGE) and identified the Gram-negative strain RX as having a very small amount of intracellular polyP (*i.e*. only a few RX cells have polyP and polyP of these cells represents only a small part of the cell volume). The RX strain was used as a "low polyP accumulator" control. RX cells were grown in PCA medium (pH 7) containing (per litre): tryptone (5.0 g); yeast extract (2.5 g) and glucose (1.0 g). The culture media were autoclaved (20 min, 121°C) and then filtered through Stericup® vacuum filtration systems with a porosity of 0.2 µm. Cultures (10 % vol/vol inoculum) were incubated at 28°C in Falcon® aerobic cell culture flasks with 0.2 µm hydrophobic membrane, in the dark, and shaken at 100 rpm. The kinetics of strain growth were monitored by measuring the optical density at 600 nm and subsequent analyses were performed during the exponential phase of growth.

### 2.2. Environmental samples

Sediment in the littoral zone of Lake Pavin (Auvergne, France) was sampled using a UWITEC (Mondsee, Austria) fitted with a polyvinyl chloride tube (1 m). The upper part (0-5 cm) of the sediment core was sampled using a sterile 50 mL pipette. To separate the microbial cells from the particles of sediment, 1 g of sediment was incubated for 30 min at 4 °C in 10 mL of sodium pyrophosphate buffer 0.01 M (pH 7.2) in a 15 mL Falcon® tube under agitation (280 rpm). The samples were placed for 1 min at 60 W in a sonication bath (Elmasonic S, Elma) and then centrifuged (2 min, 1500 g, 4 °C). The supernatant was collected and stored for 4 h at 4 °C until analysis. Water samples were collected in the water column of lake Pavin at 54 m depth with an 8-liter horizontal Van Dorn bottle, and filtered by tangential flow filtration (0.2-µm cartridge) to yield concentrate.

## 2.3. Properties of fluorescent dyes and preparation of staining solutions

4'6-diamidino-2-phenylindole (DAPI), used at a final concentration of less than 1 µg $mL^{-1}$, is a fluorescent dye that strongly binds to DNA and the DAPI-DNA complex fluoresces blue, with a maximum emission at 460 nm, after excitation by an ultraviolet (UV, 350 nm) or violet (405 nm) laser (Button and Robertson, 2001). DAPI also forms complexes with polyP when used at high concentrations (3-50 µg $ml^{-1}$, Kulakova *et al.,* 2011). DAPI-polyP complexes emit yellow-green fluorescence (525-605 nm range) when excited by a violet laser (Allan and Miller, 1980) (Fig. S1). In the present study, a stock solution of DAPI (1 mg $mL^{-1}$, *i.e*. 2.85 mM) was prepared according to the manufacturer's instructions (Thermo Fischer Scientific, Rockford, USA). The solid DAPI (powder) was redissolved in ultrapure water, aliquoted and stored at -20°C in the dark. For analysis, DAPI was diluted in the chosen buffer (HEPES, Tris-EDTA, PBS or McIlvaine, see section 2.4) before use.

The synthetic fluorochrome JC-D7 is identified as a polyP-specific marker (Angelova *et al.*, 2014). JC-D7 dye excited at 405 nm shows blue-green fluorescence emission between 480 and 510 nm (Fig. S1). In this study, stock solutions (10 mM) of JC-D7 (Chemical Cellomics Laboratory, South Korea) were prepared in dimethyl sulfoxide (molecular biology grade DMSO, Merck, Darmstadt, Germany), aliquoted and stored at -20°C in the dark. JC-D7 was diluted at 10 µM in HEPES buffer (see section 2.4) before use.

SYTO®62 fluorophore is a polymethine cyanine dye (cell permeable), that binds to nucleic acids. The DNA-SYTO®62 complex emits red fluorescence (676 nm) without spectral interaction with the polyP-DAPI or polyP-JC-D7 complexes, allowing the colocalization of DNA in PAB cells with polyP labeled with DAPI or JC-D7 (Fig. S1). In the present study, SYTO®62 stock solution (5 mM; Thermo Fischer Scientific, Rockford, USA) was stored at -20°C in the dark. For analysis, SYTO®62 was diluted at 1 µM in the chosen buffer (HEPES, Tris-EDTA, PBS or McIlvaine, see section 2.4) before use.

## 2.4. Preparation of isotonic staining buffers

The isotonic buffers used were as follows:

- Phosphate buffer saline (PBS; 1X; pH 7.2) containing per litre: NaCl (8 g); KCl (0.2 g); $Na_2HPO_4$ (1.44 g), $KH_2PO_4$ (0.24 g) and MilliQ® water.
- 4-(2-hydroxyethyl) -1-piperazine ethane sulfonic acid buffer (HEPES; 20mM, pH 7.4) containing per litre: 0.48 g of HEPES (Sigma Aldrich, CAS: 7365-45-9) and MilliQ® water.
- Tris-hydrochloride and ethylenediaminetetraacetic acid buffer (Tris-EDTA; pH 7.4) containing 10 mM Tris-HCl solution and 1mM EDTA solution (Merck KGaA, Darmstadt, Germany).
- Citrate phosphate buffer (McIlvaine; pH 7.2) containing per litre: 869.5 mL of a 0.2 M $Na_2HPO_4$ solution; 115.5 mL of a 0.1 M citric acid solution and MilliQ® water.

Buffers were sterilized by filtration on 0.2 µm (Minisart® syringe filter, Sartorius).

### 2.5. Treatments tested to define the optimum conditions for polyP staining with DAPI and sample storage conditions

To establish the optimal conditions for intracellular polyP staining, *T. elongata* (TE) and RX cell culture samples were subjected to different treatments, including different types of staining buffer (PBS, HEPES, Tris-EDTA, McIlvaine), percentages of fixative used (2 % and 4 % of formaldehyde Merck KGaA, Darmstadt, Germany), storage temperatures (4°C, -20°C, -80°C) and time (1 h and 2, 7, 14 days), and detergent addition (0 and 0.3 % triton X100, Sigma CAS: 9002-93-1). The formaldehyde is a 37 % commercial solution (CAS: 50-00-0) then diluted directly in the sample.

### 2.6. Flow cytometric (FCM) analysis of PAB after DAPI staining

The samples (final volume 200 µL) were analysed using a BD LSR Fortessa™ X-20™ flow cytometer (BD BioSciences, San Jose, CA USA) in a three lasers configuration (405 nm, 50 mW; 488 nm, 60 mW; and 640 nm, 40 mW). Samples were diluted so that the event rate was less than 3,000 cell $s^{-1}$. Fluorescence intensity, total cell number, forward scatter (FSC) and side scatter (SSC) were recorded. The fluorescence from DAPI-polyP (excitation at 405 nm) and SYTO®62-DNA (excitation at 640 nm) complexes was collected with 530/30 nm and 670/14nm bandpass filters, respectively. Data were acquired and analysed on logarithmic scales using FACSDiva™ version 9.0 (BD Biosciences).

### 2.7. Fluorescence-activated cell sorting (FACS) enrichment of polyP-containing cell stained with DAPI

We analysed a water sample collected from 54 m depth in Lake Pavin and a culture sample of fresh mixture of *T. elongata* and RX (50:50 abundance). The samples were centrifuged (4000 g, 20 min, 4°C), resuspended in PBS solution, stained with DAPI (28.5 µM, 30 min in the dark) and SYTO®62 (1 µM, 10 min) and immediately processed. Analysis and cell sorting were performed with a BD FACSAria™ Fusion SORP cell sorter equipped with a 70 µm nozzle and a 1.5 neutral density filter (BD BioSciences, San Jose, CA USA) in a three lasers configuration (405 nm, 50 mW; 488 nm, 50 mW; and 640 nm, 100 mW). A forward scatter (FSC) threshold of 200 was used, and DNA was monitored using a 640 nm excitation laser and 670/30 nm emission filter. PolyP fluorescence was monitored using a 405 nm violet laser and a 525/50 nm emission filter. Cell sorting was performed in purity mode and cells were sorted at a rate of approximately 1,500 cells $s^{-1}$ into two fractions: polyP+ (i.e. positive green fluorescence signal regarding the fluorescence intensity limit defined by the controls) and polyP-. Data were acquired and analysed on logarithmic scales using FACSDiva™ version 9.0 (BD Biosciences). Cell sorting was performed on a different machine than cell counting because the BD FACSAria™ Fusion SORP cell sorter, which is an extremely efficient cytometer for cell sorting, is cumbersome to set up. Cell counting was therefore performed on a BD LSR Fortessa™ X-20™, which is designed for this purpose. Both instruments have the same lasers and filters, making the analysis comparable, and internal quality control using fluorescent microbeads was used.

### 2.8. FCM and FACS controls

The settings for morphological (FSC and SSC) and fluorescence (DAPI, SYTO®62, JC-D7) parameters were set on the basis of samples unstained or independently stained by the different fluorochromes (SYTO®62, DAPI). Briefly, for each experiment, unstained cells were used to establish FSC and SSC signal acquisition thresholds. The minimum threshold was set for FSC only. Fluorescence thresholds for each dye (DAPI, JC-D7 and SYTO®62) were achieved by independent staining to determine where the positive and negative limits are for each. To avoid biases resulting from contamination or chemical interactions, we analysed each staining buffer alone, with each fluorochrome, or with a combination of dyes.

### 2.9. Observation by epifluorescence microscopy of intracellular polyP after labeling with DAPI

Samples were diluted with PBS (between $10^5$ and $10^6$ cells per sample), filtered through black polycarbonate membranes (0.22 µm porosity, 25 mm diameter, GTBP, Millipore®) and stained for 30 min with DAPI (28.5 µM final concentration). Filters were washed with 2 mL of PBS, incubated in the dark at 20 °C with DAPI (2.85 µM, 10 min) or SYTO®62 (1 µM, 10 min) to visualise cellular DNA. After washing with 2 mL of PBS, the filters were dried and mounted with Immersol™ immersion oil (refractive index = 1.518, Zeiss). Cells were imaged using a Zeiss™ Axio Imager 2 microscope equipped with a FLUO COLIBRI 5 source with the following light-emitting diodes: UV (385/30 nm), blue (469/38 nm), green (555/30 nm) and red (631/33 nm). The following bandpass filters were applied 450/50 nm, 525/50 nm and 690/50 nm for blue DAPI (DNA), green DAPI (polyP) and SYTO®62, respectively. The diode intensity was adjusted as follows: DAPI blue 2%; DAPI green 100%, SYTO®62 100%. PolyP and lipid inclusions are known to emit in the 450 - 650 nm range when excited at 360 nm, but lipid inclusions can be easily distinguished from polyP, as their fluorescence intensity is much lower and fades rapidly within a few seconds (Terashima *et al.*, 2020). Therefore, all photographed images were exposed to excitation light for at least 1 min prior to imaging in order to detect consistent and long-lasting bright green-yellow fluorescence from the polyP. Three replicate counts were performed for each sample (between 200 and 1000 cells per sample). Images were acquired and processed on the Zen 3.3 blue edition.

### 2.10. Transmission electron microscopy coupled with energy dispersive X-ray (TEM-EDX) spectrometry

Samples were fixed with a 2 % formaldehyde solution (final concentration) and collected on 400 mesh copper electron microscopy grids covered with a Formvar film (A03X, Pelanne Instruments, Toulouse, France) by centrifugation (18,000 g, 20 min, 14°C). After drying, the samples were observed and photographed using a JEOL JEM 2100-Plus transmission electron microscope (TEM), operating at 200 KV (JEOL Ltd, Tokyo, Japan), and equipped with a GATAN RIO 9M camera (Gatan Inc., Pleasanton, California, USA). Chemical elements were analysed in the TEM (tilted to 20°) by energy dispersive X-ray (EDX) spectrometry using the X-Max 80 $mm^2$ Large Area SDD Silicon Drift Detector (Oxford Instruments, Abingdon-on-Thames, United Kingdom) equipped with the AZtec software (Oxford Instruments, Abingdon-on-Thames, UK), in point mode or map mode.

### 2.11. Comparison of polyP staining using DAPI or JC-D7 dyes

Samples were stained with JC-D7 for polyP detection (10 µM final concentration, 30 min of incubation in the dark, Angelova *et al.*, 2014) and with SYTO®62 for DNA colocalization (1 µM, 10 min, in the dark). The treatment used as a reference was polyP staining with DAPI (28.5 µM final concentration, 30 min in the dark). The FCM analysis and controls were carried out as described in sections 2.6 and 2.8. The fluorescence of the JC-D7-polyP complexes (after excitation at 405 nm) was collected with a 530/30 nm bandpass filter (green fluorescence).

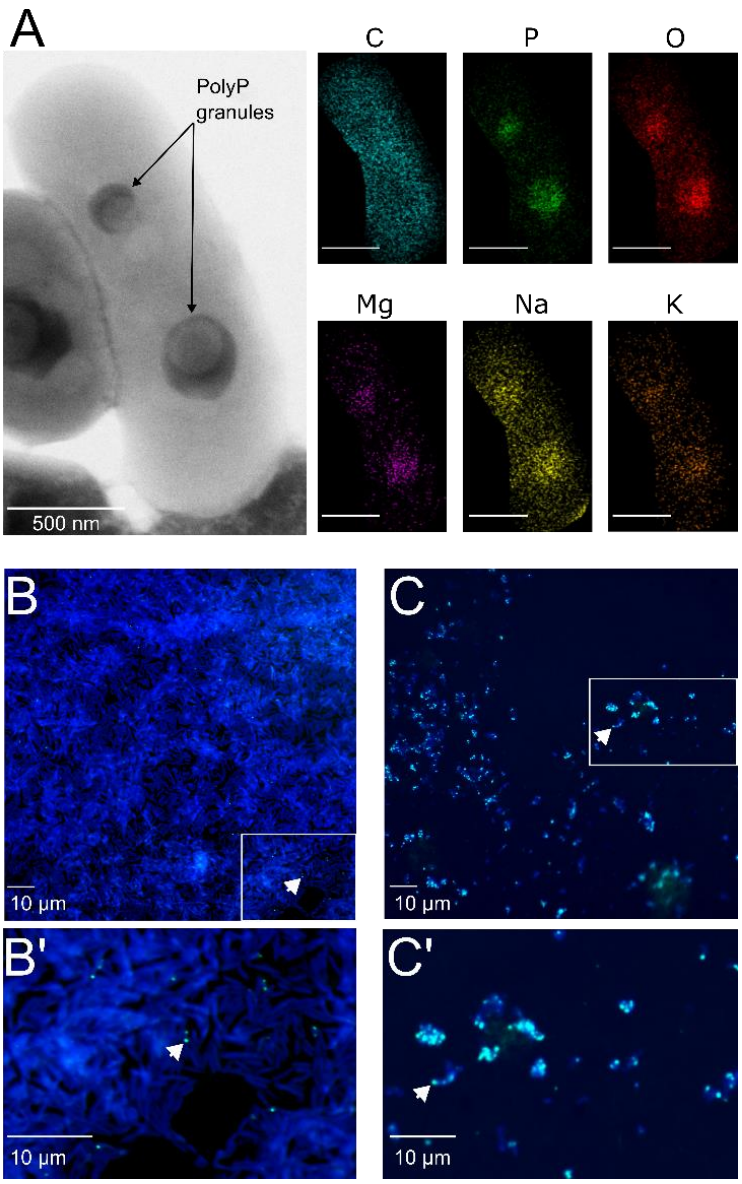


**Figure 1: Transmission electron microscopy coupled with energy dispersive X-ray spectrometry (TEM-EDX), and epifluorescence microscopy images of *T. elongata* and RX cells.**
**(A)** Representative image of two polyphosphate granules in a *Tetrasphaera elongata* Lp2 cell (DSM 14184) with EDX analysis indicating the chemical composition in and out of the granules. The elements shown are C for carbon (false blue colour), O for oxygen (false coloured in red), Na for sodium (red false colour), Mg for magnesium (false coloured in purple), P for phosphorus (green false colour), and K for potassium (false coloured in orange). Scale bars represent 500 nm (bottom left of photographs). **(B)** and **(C)** DAPI-stained images by epifluorescence microscopy of RX and *T. elongata* cells, respectively. DNA and polyP emit a blue and a green-yellow fluorescence (examples are shown by white arrows), respectively. (B') and (C') are zooms of the panels delimited by a white rectangle in images (B) and (C), respectively.

### 2.12. Statistical analyses

Statistical analyses were performed using GraphPad Prism software, version 8.0.1 for Windows (GraphPad Software, La Jolla California, USA). After Shapiro Wilk normality and Brown-Forsy homoscedasticity tests, the similarities between treatments were evaluated using a one-way ANOVA or a two-way repeated measures ANOVA, with Tukey's post-hoc test to make multiple comparisons between the groups or an unpaired t-test of Student. The data were expressed as the mean ± standard deviation of the mean (mean ± SD). A $p$ value of less than 0.05 ($p < 0.05$) was considered as statistically significant.

## 3 Results

### 3.1. Microscopy observations of polyP granules and DAPI-polyP complexes in *T. elongata* and RX cells

Transmission electron microscopy observations confirmed the presence of one or more intracellular electron-dense granules within the *T. elongata* cells (Fig.1A). Although the distribution of carbon was relatively homogeneous within cells, energy dispersive X-ray (EDX) spectrometry revealed higher amounts of P and oxygen as well as the presence of monovalent ($Na^+$, $K^+$) and divalent ($Mg^{2+}$) cations in the granules (Fig. 1A, Fig. S2).

Observations by epifluorescence microscopy revealed highly refractive granules that emit fluorescence consistent with that expected for polyP after labeling with DAPI at 28.5 µM (Fig.1B and 1C). These observations confirm that the RX strain is a low accumulator (Fig.1B and 1B'), while the *T. elongata* strain is a high accumulator (Fig. 1C and 1C') of polyP. The counting of DAPI-polyP complexes in epifluorescence microscopy will subsequently be used to validate the cytometric data.

### 3.2. Isotonic buffer for labeling polyP with DAPI in flow cytometry (FCM)

#### 3.2.1. Staining buffers versus strain populations

The effect of staining buffers on the *T. elongata* and RX strains was tested in the absence of labeling. The FSC and SSC parameters were analysed after 0, 10- and 20-min incubation of cells in the following buffers: Tris-EDTA, HEPES, PBS and McIlvaine. The Tris-EDTA buffer affected the RX population with the differentiation of a subpopulation (P2) with incubation time (Fig. 2A), suggesting that tris-EDTA damaged the cellular integrity of RX cells. Therefore, Tris-EDTA buffer was excluded from further analyses.

#### 3.2.2. Staining buffers versus SYTO®62 and DAPI dyes

The potential interference between dyes and isotonic buffers in the absence of cells was evaluated. No interference was observed between SYTO®62 and the HEPES, PBS, and McIlvaine buffers (Table S.1.). Negative controls were also validated for DAPI in PBS and HEPES buffers (Table S.2). However, artefact labeling was observed between DAPI and McIlvaine buffer (Table S.2), as evidenced by the detection of green fluorescent events in this cell-free buffer (Fig. 2B). The observed fluorescence was not linked to microbial contamination, as shown after labeling of McIlvaine buffer with SYTO®62 (Table S.1.). Therefore, the McIlvaine buffer was excluded from further analyses.

### 3.2.3. Staining buffers versus labeling performance

Cells from *T. elongata* and RX strain cultures were labeled with the fluorochrome SYTO®62 in PBS or HEPES buffer. The number of total cells counted using the fluorescence of the SYTO®62-DNA complexes was slightly higher in the HEPES buffer for both strains (Table S.3.). The same dye-buffer test was performed after labeling *T. elongata* and RX cell polyPs with DAPI. Counts were carried out in FCM and checked by epifluorescence microscopy. The proportion of *T. elongata* cells counted by FCM and containing polyP (polyP+ cells, i.e. positive green fluorescence signal regarding the fluorescence intensity limit defined by the controls) over the total cells was 82.3 ± 0.2 % and 87.5 ± 0.1 % in PBS and HEPES buffer, respectively (Table S.4).

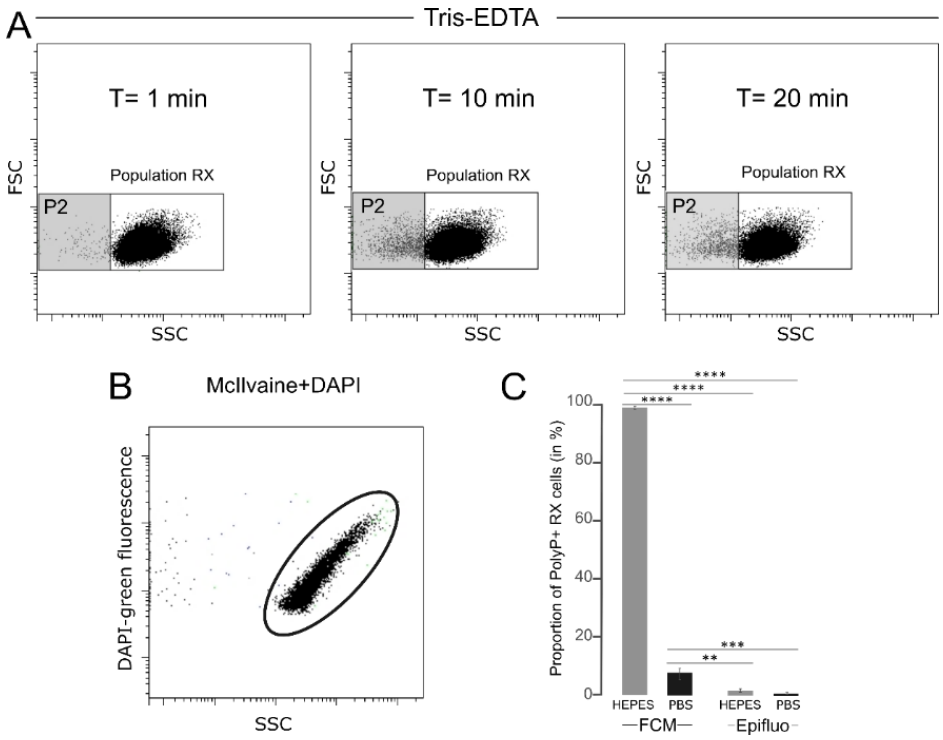


**Figure 2: Tests of different isotonic buffers for the labeling of polyP with DAPI in flow cytometry**
**(A)** Cytograms obtained after T=1 min, T=10 min and T=20 min incubation of unlabeled RX cells in Tris-EDTA buffer. **(B)** Cytogram obtained after DAPI labeling of McIlvaine buffer without cells revealing an artefact signal with green fluorescence. (**C**) Proportion of polyP+ cells counted by flow cytometry (FCM) or epifluorescence microscopy (Epifluo) after labeling RX cells with DAPI in HEPES or PBS buffer. Significance was determined using one-way ANOVA test and Tukey's post-hoc test for multiple comparisons denoted as follows: $^{*}p<0.05$, $^{**}p < 0.001$, $^{***}p < 0.0005$, and $^{****}p < 0.0001$.
FSC: forward scatter, SSC: Side scatter

The controls performed by epifluorescence microscopy after labeling the *T. elongata* cells with DAPI confirmed these proportions with polyP+ cells accounting for 87.2 ± 5.5 % and 92.5 ± 2.9 %, in PBS and HEPES buffer, respectively (Table S.5). Regardless of the counting method (FCM or epifluorescence microscopy) or buffer (HEPES or PBS), the results for the *T. elongata* strain are consistent (Table S.6). On the other hand, the proportions of polyP+ cells detected in RX cultures diluted in HEPES (99.9 ± 0.0 %) or PBS (7.2 ± 2.4%) buffer and counted by FCM were very different (Fig. 2C, Table S.7). The control count performed by epifluorescence microscopy (1.9 ± 1 % and 0.9 ± 0.5 % for PBS and HEPES, respectively, Table S.8), although significantly different (Table S.9) from the FCM, showed that the proportion was in the similar range to that obtained in the PBS buffer using FCM (Fig. 2C). Therefore, HEPES buffer which results in artefactual labeling for the Gram-negative RX strain, was excluded and PBS buffer was used for subsequent FCM and FACS analyses.

### 3.3. Permeabilisation and storage conditions

#### 3.3.1. Cell permeabilisation

To assess the degree of permeability on the efficiency of polyP labeling, RX and *T. elongata* cells were pretreated with a synthetic detergent, triton X-100, or a fixative, formaldehyde. As revealed by cytometry data after labeling with SYTO®62, cell incubation in 0.3 % triton X-100 induced a cell loss of 43.5 ± 5.2 % and 62.7 ± 5.2 % for *T. elongata* and RX, respectively (Table S.10). After 1 h of incubation (T0), fixation with formaldehyde at a final concentration of 2 or 4 % had a significant impact on the detection of polyP+ cells for the RX strain compared with the unfixed culture (Fig. 3A, Table S.11 and S.12). No significant difference in the proportion of polyP+ cells was observed for *T. elongata* fixed with 2 % and 4 % formaldehyde compared to unfixed cells (Fig. 3B, Table S.13 and S.14).

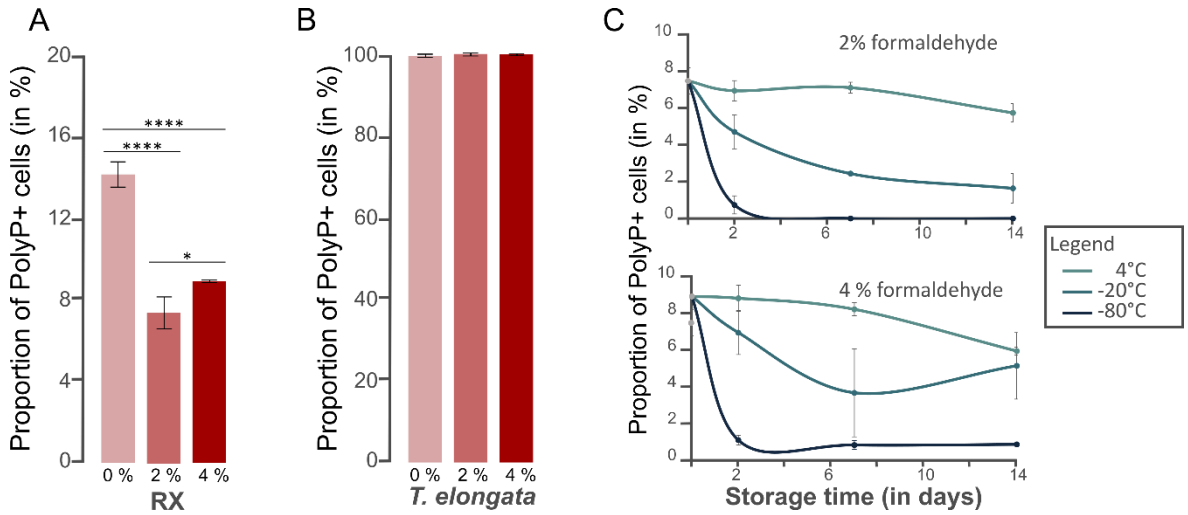


**Figure 3: Preservation of PolyP+ as a function of formaldehyde concentration, temperature and storage time**
Proportion of polyP+ cells detected in the **(A)** RX and **(B**) *T. elongata* strain cultures at day 0 without addition of fixative (0%) and with 2% and 4% formaldehyde. Significance was determined using one-way ANOVA test, and Tukey's post-hoc test for multiple comparisons, denoted as follows: $^{*}p < 0.05$, and $^{****}p < 0.0001$. **(C)** Proportion of polyP+ cells detected in the RX strain culture after fixation at 2% (top graph) or 4% (bottom graph) as a function of storage time (2, 7 and 14 days) and storage temperature (4°C, -20°C, -80°C).

#### 3.3.2. Cell preservation

PolyP preservation was assessed after formaldehyde fixation at 2 or 4 % by investigating the proportion of polyP+ cells detected after different storage times (t = 2, 7 and 14 days) and temperatures (4 °C, -20 °C, -80 °C) (Table S.11 and S.13). No significant difference was observed for *T. elongata* strain, whatever the formaldehyde concentration, storage time or temperature (Table S.15). However, storage at -20°C or -80°C is not optimal for the RX strain, whatever the fixative concentration (Fig. 3C and 3D, Table S.16 and S.17). For this Gram-negative strain, storage at 4°C after fixation with 2% formaldehyde is the most suitable storage condition.

### 3.4. Validation of the DAPI-labeling protocol for polyP for FACS analyses

First, we prepared a mixed culture of *T. elongata* and RX. After determining the number of RX and *T. elongata* cells in each strain culture by FCM and SYTO®62 labeling, we mixed them in a 50:50 abundance ratio. Fluorescence-activated cell sorting (FACS) was performed on this 50:50 mixture (Fig. 4A). We determined the proportion of polyP+ cells by counting them by epifluorescence microscopy and FCM, after labeling with DAPI, prior to cell sorting (Fig. 4B). We also carried out these counts using these two approaches after cell sorting in each of the polyP+ (Fig. 4C) and polyP- fractions (Fig.4D) (Table S.18).

Prior to cell sorting, 36.5 % and 12.6 ± 7.5 % of cells were identified as polyP+ in the mixed *T. elongata* +RX culture by FCM and epifluorescence microscopy, respectively (Fig. 4B, Table S.18). After cell sorting, $4.5.10^6$ and $4.3.10^6$ cells were collected in the polyP+ and polyP- (i.e. negative green fluorescence signal regarding the fluorescence intensity limit defined by the controls) fractions, respectively (Fig. 4C and 4D). A strong enrichment of PAB was observed in the polyP+ fraction, as shown by FCM and epifluorescence microscopy counts (> 80 % of polyP+ cells, Fig. 4E, Table S.18). In contrast, PAB represented less than 15 % in the polyP- fraction (Fig. 4F, Table S.18).

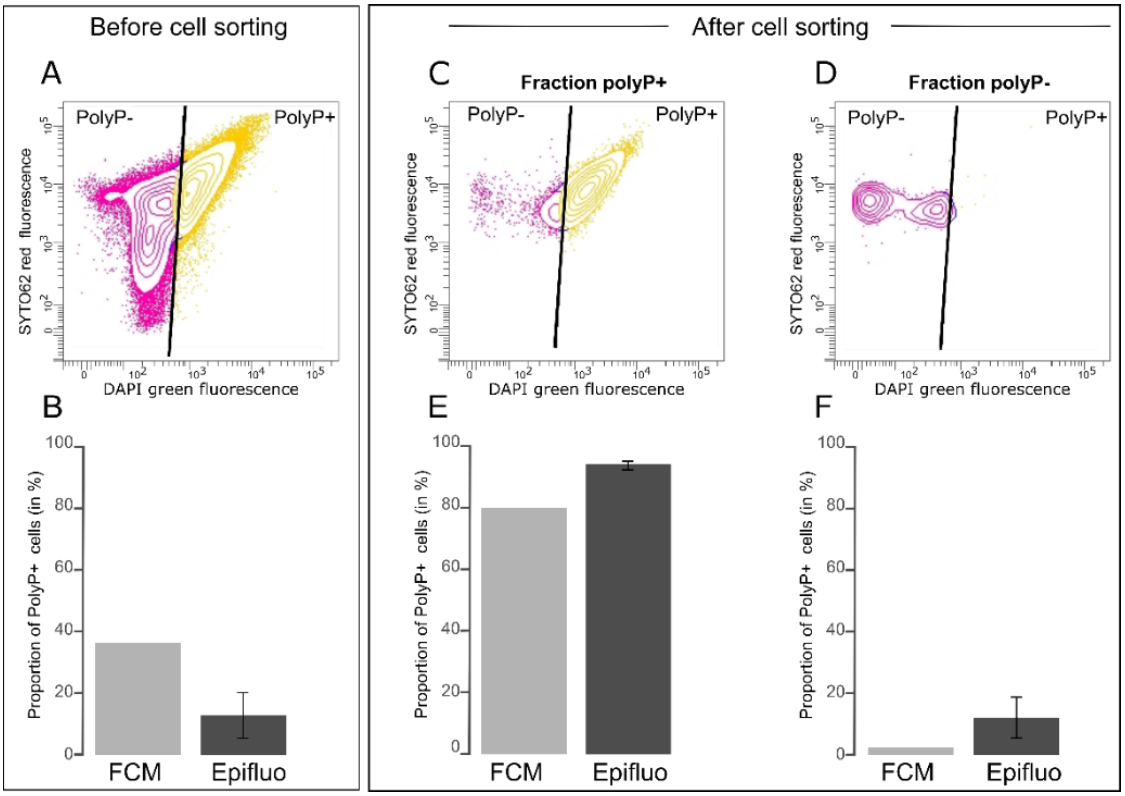


**Figure 4: PAB cell sorting from a mixed culture of *T. elongata* and RX**
**(A)** Cytogram showing the fluorescence of polyP-DAPI complexes (green fluorescence) and the fluorescence of DNA-SYTO®62 complexes (red fluorescence) in the mixed culture of *T. elongata* and RX prior to cell sorting.
**(B)** Proportion of polyP+ cells in the mixed culture of *T. elongata* and RX, labeled with DAPI prior to cell sorting and counted by flow cytometry (FCM) and epifluorescence microscopy (Epifluo).
**(C)** and **(D)** Cytograms showing the fluorescence of polyP-DAPI complexes (green fluorescence) and the fluorescence of DNA-SYTO®62 complexes (red fluorescence) in the **(C)** polyP+ and **(D)** polyP- fraction after cell sorting of the mixed culture of *T. elongata* and RX.
**(E)** and **(F)** Proportion of polyP+ cells in fractions **(C)** polyP+ and **(D)** polyP- after cell sorting of the mixed culture of *T. elongata* and RX and counted by flow cytometry (FCM) and epifluorescence microscopy (Epifluo).
Standard deviations are not shown for FCM because only one sample was counted per fraction.

Cell sorting after labeling of polyP with DAPI and DNA with SYTO®62 was also carried out on a lake water sample (Table S.19). Cells from the water sample were sorted by FACS and 7.9 x $10^6$ and 6.3 x $10^6$ cells were collected in the polyP+ and polyP- fractions, respectively. PolyP+ cells were counted by epifluorescence microscopy before and after cell sorting (Table S.19). Prior to cell sorting, the water sample contained 9.7 ± 1.5 % of polyP+ cells (Table S.19) Target cells enrichment was observed in the polyP+ fraction, with 52 ± 1.8 % of polyP+ cells (Table S.19). Although highly significant ($p < 0.0001$), this enrichment was much less effective than that obtained with the mixture of RX+TE strains (Fig. 4).

### 3.5. Counting of PAB from strain cultures and environmental samples using DAPI or JC-D7 labeling

Tests were carried out using the JC-D7 dye, known to be specific for polyPs, in parallel with DAPI labeling. The green fluorescence intensity of JC-D7 at 525 nm, was lower than that of DAPI (Fig.S3). Culture samples of *T. elongata* and RX strains and lake sediments were labeled with DAPI or JC-D7 for polyP and SYTO®62 for DNA. The proportion of polyP+ cells was counted in FCM and control counts, on the same samples, were carried out using epifluorescence microscopy (Table S.20 to S.22). For RX and *T. elongata* strains, as observed previously (Fig. 4), the DAPI-labeled polyP+ cell counts, although showing significant differences between FCM and epifluorescence microscopy, were in similar proportions (Fig. 5). For the *T. elongata* strain, the proportion of polyP+ cells after polyP labeling with JC-D7 fluorochrome (93.7 ± 1.5 %) was not significantly different from that determined by epifluorescence microscopy (96.3 ± 1.9 %, Fig. 5, Table S.20). For RX strain, the proportions of polyP+ determined by FCM after labeling with JC-D7 (4.8 ± 0.3 %) or DAPI (5.8 ± 0.5 %) were not significantly different (Fig. 5, Table S.21). However, these proportions were significantly lower than those obtained after counting by epifluorescence microscopy (12.3 ± 1.2 %, Fig. 5, Table S.21). For the lake sediment sample, JC-D7 and DAPI fluorochromes led to a very different detection of polyP+ cells by FCM (82.8 ± 2.3 % and 5 ± 0.1% polyP+ cells for DAPI and JC-D7, respectively, Fig. 5, Table S.22). Control counts by epifluorescence microscopy (10.5 ± 7.2 %) were not significantly different from FCM counts after labeling with JC-D7 (Fig. 5, Table S.22).

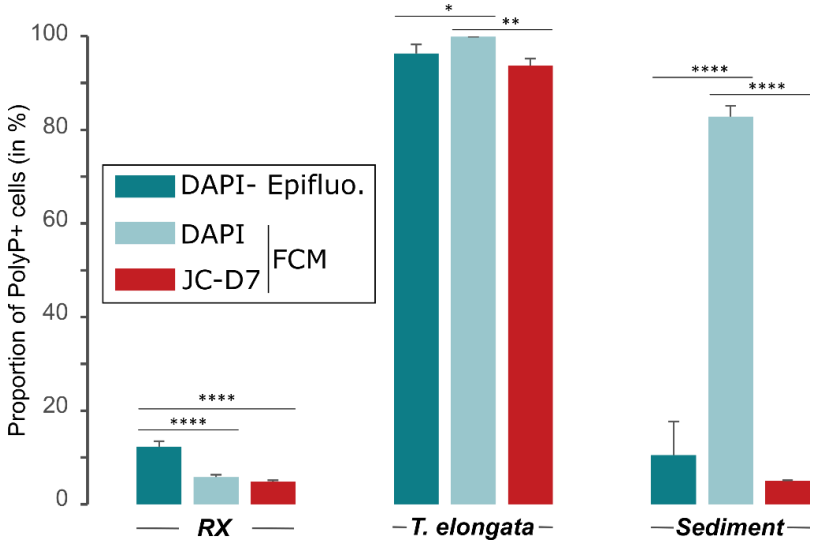


**Figure 5: Comparison of JC-D7 and DAPI labeling for PAB detection**
Proportion of polyP+ cells, after PAB labeling with DAPI and SYTO®62 or with JC-D7 and SYTO®62. Cells were counted by flow cytometry (FCM) or epifluorescence microscopy (Epifluo). Significance was determined using one-way ANOVA test and Tukey's post-hoc test for multiple comparisons, denoted as follows: $^{*}p < 0.05$, $^{**}p < 0.001$, $^{***}p < 0.0005$, and $^{****}p < 0.0001$.

## 4 Discussion

### 4.1. Optimisation of polyP labeling with DAPI

The coupling of specific polyP detection to flow cytometry has been used in a very small number of studies that have applied standardised conditions previously defined in the literature, for example, for polyP detection by epifluorescence microscopy (e.g. Mesquita *et al.*, 2013; Voronkov *et al.*, 2019). In this study, we tested several variables likely to affect the efficiency and reliability of PAB detection in the environment. These variables, which include the choice of buffer, fluorochrome or fixative concentration, may seem trivial but they are essential for defining future standardized protocols and should be acquired as a priority. This will enable the scientific community to avoid pitfalls and save time and effort in carrying out tedious analyses.

Our data show that the parameters for labeling polyP with DAPI are not necessarily transposable from *ad hoc* conditions adapted to epifluorescence microscopy and that specific adaptation of the labeling methods is required for the flow cytometry approach. For example, McIlvaine buffer, which has been identified to significantly enhance DAPI-polyP labeling in epifluorescence microscopy (Mukherjee and Ray, 2015), causes events with size and structure mimic nonviable cells. These artefact signals observed, linked to McIlvaine-DAPI interactions whose physicochemical origin has not been identified, are highlighted by flow cytometry. In contrast, the intense fluorescence of green DAPI when cells were labeled in HEPES buffer suggests that the latter is an optimal solvent for the detection of polyP by flow cytometry. However, this fluorescence detection was artefactual and led to an overestimation of the proportion of polyP+ cells within the Gram-negative RX population as revealed by epifluorescence microscopy observations on the same samples. A possible explanation could be that HEPES leads to erroneous measurements of fluorescence parameters assessed by flow cytometry due to strong alterations of the bacterial membrane owing to the composition of this buffer (e.g. lack of divalent cations, Tomasek *et al.* 2018). This buffer is not optimal for diluting the Gram-negative RX strain, and potentially Gram-negative bacteria in general, for the detection and quantification of polyP+ cells. This effect was not identified for the Gram-positive *T. elongata* strain suggesting that the artefact observed is due to membrane properties. This study thus provides convincing evidence that the choice of buffer for labeling polyP with DAPI should be PBS, which is also a frequently used buffer for labeling DNA with this fluorochrome.

In addition, we show that membrane permeabilisation steps are not necessary for the detection of polyP by DAPI labeling in FCM. On the contrary, significant losses were recorded in terms of the total number of events and proportions of polyP+ cells with two compounds, a detergent (triton X100) and a fixative (formaldehyde), which have different modes of action but both permeabilize cell membranes. In order to reconcile this methodological approach with the constraints of environmental studies, which often do not allow samples to be analysed immediately, the conservation of polyP was considered. The bias induced immediately after formaldehyde fixation for the detection of PAB did not increase significantly after samples were stored for 14 days at 4°C for RX and for all storage temperatures for *T. elongata*. Consequently, we recommend storage, after fixation with 2% formaldehyde, at 4°C. This temperature avoids freeze-thaw cycles that could damage cells during repeated analyses of the same sample. It is also compatible with transporting samples from the sampling site under *ad hoc* conditions.

We also simultaneously applied DNA-SYTO®62 labeling and polyP-DAPI labeling. This double labeling, which has not been used in previous studies (*e.g.*, Günther *et al.* 2009; Terashima *et al.*, 2020), enables the separation of

PAB from common autofluorescent contaminants such as aggregates or organic matter. In addition, the choice of SYTO®62 avoids interference with the metachromatic properties of DAPI by using a fluorochrome whose emission spectra are perfectly separable from the green and blue fluorescence of DAPI.

### 4.2. Is polyP labeling with DAPI really applicable to FCM in environmental samples?

Controls on the number of polyP cells counted by FCM were carried out by epifluorescence microscopy, a standard method for quantifying and visualizing PAB (Serafim *et al*., 2002). In almost all the data obtained, the observations by FCM and epifluorescence are significantly different, and especially in natural samples, the differences were striking. Should FCM therefore be recommended for the detection of DAPI-labeled polyPs? DAPI is an inexpensive dye for which most epifluorescence microscopes and flow cytometers have combinations of excitation and emission filters compatible with the detection of its blue or green fluorescence (e.g. Tarayre *et al.*, 2016). However, DAPI is also a nonspecific polyP dye. In addition to labeling DNA (blue fluorescence), it also interacts with lipids, displaying metachromatic properties similar to those of polyP (Serafim *et al.*, 2002). Although the DAPI-lipid fluorescence is short-lived, with respect to the speed of flow cytometry analysis, it cannot be ignored whereas in microscopy the longer exposure times for counting make it possible to avoid the artefactual counting of lipids.

Nevertheless, FCM and epifluorescence microscopy are different methods. The main advantage of flow cytometry is its counting speed, which makes it possible to establish the proportions of PAB in a large sample of cells from the targeted microbial community or population. Microscopy, in turn, allows visualization of the research material but does not count many cells (generally up to 400; Kepner and Pratt, 1994) and often depends on the experimenter. Since the basic assumption of most statistical tests is that samples are randomly and independently selected, the approach of randomly selecting fields of view or squares of an ocular graticule to count bacteria is generally practised in epifluorescence microscopy (Kirchman *et al.* 1982). However, this approach has been shown to produce a significant statistical bias, contributed for example to 60-80 % of the total variance in bacteria count data for seawater samples (Kirchman *et al.* 1982). This could be explained by the fact that the actual distribution of bacterial cells in environmental samples may not be random and thus contribute to the overestimation or underestimation of total bacterial abundance.

However, and despite the substantial variation and subjectivity associated with microscopy and flow cytometry, both methods revealed, in the case of appropriate labeling (e.g. appropriate staining buffer), the proportions of polyP+ cells in a rather congruent manner for homogeneous samples, i.e. *T. elongata* and RX strain samples. The method combining FCM and DAPI labeling of polyPs can therefore be applied to ‘simple’ matrices, for example to screen a heterogeneous pool of cells or a single strain for gene-phenotype linkage analyses.

The use of flow cytometry combined with DAPI staining of polyP for counting PAB in complex matrices, such as sediment or freshwater samples, cannot however be recommended due to the obvious differences between FCM and epifluorescence counts. However, although the FCM-DAPI labeling approach is not reliable for PAB counts in complex samples, our results confirm that PAB can be enriched from the environmental microbial community using FACS and DAPI-PolyP labeling, which opens up very interesting prospects. Terashima *et al.* (2020) have demonstrated that ~70% of cells remain viable after DAPI staining, enabling effective enrichment and isolation of PAB after FACS-based phenotype screening. This ‘targeted enrichment’ may also be combined with

metagenomics (Thompson *et al.* 2013) to improve recovery of metagenome-assembled genomes of environmental PAB.

### 4.3 The polyP specific fluorochrome JC-D7 as a prospective marker for complex environmental samples

Considering that DAPI labeling is not suitable for enumerating PAB in environmental samples due to the non-specificity of this fluorochrome, the best option would therefore be to use markers specific to polyP. This approach was advocated by Gunther *et al.* (2002) who proposed using the bright green fluorescence of the antibiotic tetracycline when it complexes divalent cations acting as a countercharge in polyphosphate granules. Prior to the study presented here, we had carried out assays by labeling cultured strains and/or environmental samples with tetracycline but had not obtained convincing results.

Therefore, an exploratory analysis was performed to determine the potential of a heterocycle of the benzimidazole family for the detection of PAB in flow cytometry. The JC-D7 dye, identified as specific to polyP, has never been used to target PAB, but only for staining polyP in living eukaryotic cells and tissues (Angelova *et al.*, 2014). The JC-D7 dye was shown to allow for specific labeling of synthetic polyP *in vitro* as well as endogenous polyP in living mammalian cells which have a dramatically lower abundance of polyP when comparing to microorganisms. In addition, this probe demonstrated high selectivity for the labeling of polyP that was not sensitive to a number of ubiquitous organic polyphosphates, notably RNA (Angelova *et al*. 2014). The data obtained in the present study show that the counts made with JC-D7 in FCM on environmental samples were not statistically different from those made by epifluorescence microscopy after labeling with DAPI. JC-D7 looks promising for the use in natural samples and its relevance to the study of PAB needs to be confirmed by further studies. An important next step will be to demonstrate the specific nature of the JC-D7 labeling of PAB by and will require fluorescence microscopy to visualize the JC-D7 dye in combination with, for instance, scanning-electron microscopy combined with energy dispersive spectroscopy (SEM-EDS) to perform co-localisation analysis. Developing a protocol for staining polyP with the JC-D7 probe using epifluorescence microscopy will require further development, particularly due to the weaker fluorescence of JC-D7 compared with DAPI that we demonstrated in our study. The development of cytometry methods, in particular spectral cytometry, could also allow co-labeling of DAPI and JC-D7. This approach is currently impossible with conventional cytometry because the spectra of polyP DAPI and JC-D7 overlap and the acquisition wavelengths are very close (520 nm and 530 nm respectively).

## References


Akbari A., Wang, Z., He, P., Wang, D., Lee, J., Han I. L., Li, G., and Gu, A. Z.: Unrevealed roles of polyphosphate-accumulating microorganisms. Microb. Biotechnol., 14, 82-87, doi: 10.1111/1751-7915.13730, 2021.

Allan, R. A., and Miller, J. J. : Influence of s-adenosylmethionine on DAPI-induced fluorescence of polyphosphate in the yeast vacuole. Can. J. Microbiol., 26, 912-920, doi.org/10.1139/m80-158, 1980.

Angelova, P.R., Agrawalla, B.K., Elustondo, P.A., Gordon, J., Shiba, T., Abramov, A.Y., Chang, Y.-T., and Pavlov, E.V.: In situ investigation of mammalian inorganic polyphosphate localization using novel selective fluorescent probes JC-D7 and JC-D8. ACS Chem. Biol., 9, 2101–2110, doi.org/10.1021/cb5000696, 2014.

Bennett, E. M., Carpenter, S. R., and Caraco, N. F.: Human impact on erodable phosphorus and eutrophication: a global perspective: increasing accumulation of phosphorus in soil threatens rivers, lakes, and coastal oceans with eutrophication. BioScience, 51, 227–234, doi.org/10.1641/0006-3568(2001)051[0227:HIOEPA]2.0.CO;2, 2001.

Bidaud, C. C., Monteil, C. L., Menguy, N., Busigny, V., Jézéquel, D., Viollier, E., Travert, C., Skouri-Panet, F., Benzerara, K., Lefevre C. T., Duprat E.: Biogeochemical Niche of Magnetotactic Cocci Capable of Sequestering Large Polyphosphate Inclusions in the Anoxic Layer of the Lake Pavin Water Column. Front Microbiol., 12, doi.org/10.3389/fmicb.2021.789134, 2022.

Brown, M. R. W., and Kornberg, A. Inorganic polyphosphate in the origin and survival of species. Proc Nat Acad Sci., 101, 16085–16087, doi: 10.1073/ pnas.0406909101, 2004.

Button, D. K., and Robertson, B. R.: Determination of DNA content of aquatic bacteria by flow cytometry. Appl Environ Microbiol, 67,1636-45, doi: 10.1128/AEM.67.4.1636-1645.2001, 2001.

Cordell, D., Drangert, J. -O., and White, S.: The story of phosphorus: Global food security and food for thought. Glob. Environ. Change, 19, 292–305, doi.org/10.1016/j.gloenvcha.2008.10.009, 2009.

Cordell, D., Rosemarin, A., Schröder, J. J., and Smit, A. L.: Towards global phosphorus security: A systems framework for phosphorus recovery and reuse options. Chemosphere, 84, 747-758, doi: 10.1016/j.chemosphere.2011.02.032, 2011.

Cosmidis, J., Benzerara, K., Morin, G., Busigny, V., Lebeau, O., Jézéquel, D., Noel, V., Dublet A. G., Othmane, G.: Biomineralization of iron-phosphates in the water column of Lake Pavin (Massif Central, France), Geoch. Cosmoch. Acta, 126, 78-96. 10.1016/j.gca.2013.10.037, 2014.

Diaz, J., Ingall, E., Benitez-Nelson, C., Paterson, D., de Jonge, M. D., McNulty, I., and Brandes, J. A.: Marine polyphosphate: a key player in geologic phosphorus sequestration. Science, 320, 652-655, doi:10.1126/science.1151751, 2008.

Diaz, R. J., and Rosenberg, R.: Spreading dead zones and consequences for marine ecosystems. Science, 321, 926–929, doi :10.1126/science.1156401, 2008.

Falkowski, P., Scholes, R. J., Boyle, E., Canadell, J., Canfield, D., Elser, J., Gruber, N., Hibbard, K., Högberg, P., Linder, S., Mackenzie, T., Moore III, B., Rosenthal, Y., Seitzinger, S., Smetacek, V., and Steffen, W.: The global carbon cycle: a test of our knowledge of earth as a system. Science, 290, 291-296, doi:10.1126/science.290.5490.291, 2000.

Fernando, E.Y., McIlroy, S.J., Nierychlo, M., Herbst, F-A., Petriglieri, F., Schmid, M. C., Wagner, M., Nielsen, J. L., and Nielsen, P. H. Resolving the individual contribution of key microbial populations to enhanced biological phosphorus removal with Raman–FISH. ISME J, 13, 1933-1946, https://doi.org/10.1038/s41396-019-0399-7, 2019.

Günther, S., Trutnau, M., Kleinsteuber, S., Hause, G., Bley, T., Röske, I., Harms, H., and Müller, S. Dynamics of polyphosphate-accumulating bacteria in wastewater treatment plant microbial communities detected via DAPI (4',6'-diamidino-2-phenylindole) and tetracycline labeling. Appl Environ Microbiol, 75, 2111-2121, doi:10.1128/AEM.01540-08, 2009.

Kepner, R.L., Pratt, J.R. Use of fluorochromes for direct enumeration of total bacteria in environmental samples: past and present. Microbiol Rev, 58, 603-615, https://doi.org/10.1128/mr.58.4, 1994.

Kirchman, D., Sigda, J., Kapuscinski, R., and Mitchell, R. Statistical analysis of the direct count method for enumerating bacteria. Appl Environ Microb, 44, 376-382, https://doi.org/10.1128/aem.44.2.376-382, 1982.

Kornberg, A., Rao, N. N., and Ault-Riché, D. Inorganic polyphosphate: a molecule of many functions. Annu Rev Biochem 68, 89-125, doi: 10.1146/ annurev.biochem.68.1.89, 1999.

Kulakova, A. N., Hobbs, D., Smithen, M., Pavlov, E., Gilbert, J. A., Quinn, J. P., and McGrath, J. W.: Direct quantification of inorganic polyphosphate in microbial cells using 4'-6-diamidino-2-phenylindole (DAPI). Environ. Sci. Technol. 45, 7799-7803, doi.org/10.1021/es201123r, 2011.

Lorenzo-Orts, L., Couto, D., Hothorn, M.: Identity and functions of inorganic and inositol polyphosphates in plants. New Phytologist 225, 637-652, doi: 10.1111/nph.16129, 2020.

Majed, N., Li, Y., and Gu, A. Z. Advances in techniques for phosphorus analysis in biological sources. Current Opinion in Biotechnology, 23, 852-859, https://doi.org/10.1016/j.copbio.2012.06.002, 2012.

Martin, P., Dyhrman, S. T., Lomas, M. W., Poulton, N. J., and van Mooy, B. A. S.: Accumulation and enhanced cycling of polyphosphate by Sargasso Sea plankton in response to low phosphorus. PNAS 111, 8089– 8094, doi: 10.1073/pnas.1321719111, 2014.

Martin, P., and Van Mooy, B. A. S. Fluorometric quantification of polyphosphate in environmental plankton samples: extraction protocols, matrix effects, and nucleic acid interference. Appl Environ Microbiol 79, https://doi.org/10.1128/AEM.02592-12, 2013.

Mesquita, D. P., Amaral, A. L., and Ferreira, E. C.: Activated sludge characterization through microscopy: A review on quantitative image analysis and chemometric techniques. Anal. Chim. Acta, 802, 14-28, doi.org/10.1016/j.aca.2013.09.016, 2013.

Mukherjee, C., and Ray, K.: An improved DAPI staining procedure for visualization of polyphosphate granules in cyanobacterial and microalgal cells. Protocol Exchange. 10 (4075), doi:10.1038/protex.2015.066, 2015.

Nguyen, H. T., Le, V. Q., Hansen, A. A., Nielsen, J. L., and Nielsen, P. H. High diversity and abundance of putative polyphosphate-accumulating Tetrasphaera-related bacteria in activated sludge systems. FEMS Microbiol Ecol, 76, 256-67, doi: 10.1111/j.1574-6941.2011.01049.x, 2011.

Rao, N. N., Gómez-García, M. R., and Kornberg, A. Inorganic polyphosphate: essential for growth and survival. Annu Rev Biochem 78, 605-647, doi: 10.1146/annurev.biochem.77.083007.093039, 2009.

Rivas-Lamelo, S., Benzerara, K., Lefèvre, C. T., Monteil, C. L., Jézéquel, D., Menguy, N., Viollier, E., Guyot, F., Férard, C., Poinsot, M., Skouri-Panet, F., Trcera, N., Miot, J., and Duprat, E.: Magnetotactic bacteria as a new model for P sequestration in the ferruginous Lake Pavin. Geochem Perspect Lett, 5, 35-41, doi: 10.7185/geochemlet.1743, 2017.

Serafim, L. S., Lemos, P. C., Levantesi, C., Tandoi, V., Santos, H., and, Reis, M. A. M.: Methods for detection and visualization of intracellular polymers stored by polyphosphate-accumulating microorganisms, J. Microbiol. Methods 51, 1-18, doi.org/10.1016/S0167-7012(02)00056-8, 2002.

Tarayre, C., Nguyen, H. T., Brognaux, A., Delepierre, A., De Clercq, L., Charlier, R., Michels, E., Meers, E., and Delvigne, F. Characterization of phosphate accumulating organisms and techniques for polyphosphate detection: a review. Sensors 16, 797, doi.org/10.3390/s16060797, 2016.

Terashima, M., Kamagata, Y., and Kato, S.: Rapid enrichment and isolation of polyphosphate accumulating organisms through 4'6-Diamidino-2-Phenylindole (DAPI) staining with fluorescence-activated cell sorting (FACS). Front. Microbiol. 11. doi.org/10.3389/fmicb.2020.00793, 2020.

Tomasek, K., Bergmiller, T., Guet, C. C. Lack of cations in flow cytometry buffers affect fluorescence signals by reducing membrane stability and viability of Escherichia coli strains. J Biotechnol, 268:40-52, doi: 10.1016/j.jbiotec.2018.01.008, 2018.

Thompson, A., Bench, S., Carter, B., Zehr, J. Coupling FACS and genomic methods for the characterization of uncultivated symbionts, In Methods in Enzymology, E. F. DeLong (Eds.), Academic Press, 531, 45-60, https://doi.org/10.1016/B978-0-12-407863-5.00003-4, 2013

Voronkov, A., and Sinetova, M. Polyphosphate accumulation dynamics in a population of *Synechocystis* sp. PCC 6803 cells under phosphate overplus. Protoplasma 256, 1153-1164, doi.org/10.1007/s00709-019-01374-2, 2019.

Zilles, J. L., Peccia, J., Kim, M. W., Hung, C. H., and Noguera, D. R. Involvement of Rhodocyclus-related organisms in phosphorus removal in full-scale wastewater treatment plants. Appl. Environ. Microbiol., 68, 2763-2769, doi: 10.1128/AEM.68.6.2763-2769.2002, 2002.

**Author contribution**

CB, HB, CCB, KB, F S-P, ED and ACL designed the work. CB, HB, Y-T C and ACL designed the experiments. ED was responsible for the research project (ANR Phostore). CB, HB, CCB, JC and ACL carried out the experiments. ACL, CB and HB wrote the manuscript and all the authors revised it.

**Competing interest**

The authors declare that they have no conflict of interest

**Acknowledgments**

Clémentin Bouquet was supported by PhD fellowship from the French Ministry of Education and Research. Cécile Bidaud was supported by the Ecole Doctorale FIRE-Programme Bettencourt. The authors would also like to thank Christopher Lefevre (BIAM, UMR 7265, CEA Cadarache) and Nicolas Menguy (IMPMC, UMR CNRS 7590, Sorbonne university). This work was supported by the Agence Nationale de la Recherche (PHOSTORE: ANR-19-CE01-0005). Young-Tae Tchang was supported by the National Research Foundation of Korea (NRF) grant funded by the Korea government (MSIT) (2023R1A2C300453411)

**Legends of figures**

**Figure 1: Transmission electron microscopy coupled with energy dispersive X-ray spectrometry (TEM-EDX), and epifluorescence microscopy images of *T. elongata* and RX cells.**
**(A)** Representative image of two polyphosphate granules in a *Tetrasphaera elongata* Lp2 cell (DSM 14184) with EDX analysis indicating the chemical composition in and out of the granules. The elements shown are C for carbon (false blue colour), O for oxygen (false coloured in red), Na for sodium (red false colour), Mg for magnesium (false coloured in purple), P for phosphorus (green false colour), and K for potassium (false coloured in orange). Scale bars represent 500 nm (bottom left of photographs). **(B)** and **(C)** DAPI-stained images by epifluorescence microscopy of RX and *T. elongata* cells, respectively. DNA and polyP emit a blue and a green-yellow fluorescence (examples are shown by white arrows), respectively. (B') and (C') are zooms of the panels delimited by a white rectangle in images (B) and (C), respectively.

**Figure 2: Tests of different isotonic buffers for the labeling of polyP with DAPI in flow cytometry**
**(A)** Cytograms obtained after T=1 min, T=10 min and T=20 min incubation of unlabeled RX cells in Tris-EDTA buffer. **(B)** Cytogram obtained after DAPI labeling of McIlvaine buffer without cells revealing an artefact signal with green fluorescence. (**C**) Proportion of polyP+ cells counted by flow cytometry (FCM) or epifluorescence microscopy (Epifluo) after labeling RX cells with DAPI in HEPES or PBS buffer. Significance was determined

using one-way ANOVA test and Tukey's post-hoc test for multiple comparisons denoted as follows: $^{*}p<0.05$, $^{**}p < 0.001$, $^{***}p < 0.0005$, and $^{****}p < 0.0001$.

FSC: forward scatter, SSC: Side scatter

**Figure 3: Preservation of PolyP+ as a function of formaldehyde concentration, temperature and storage time**

Proportion of polyP+ cells detected in the **(A)** RX and **(B**) *T. elongata* strain cultures at day 0 without addition of fixative (0%) and with 2% and 4% formaldehyde. Significance was determined using one-way ANOVA test, and Tukey's post-hoc test for multiple comparisons, denoted as follows: $^{*}p < 0.05$, and $^{****}p < 0.0001$. **(C)** Proportion of polyP+ cells detected in the RX strain culture after fixation at 2% (top graph) or 4% (bottom graph) as a function of storage time (2, 7 and 14 days) and storage temperature (4°C, -20°C, -80°C).

**Figure 4: PAB cell sorting from a mixed culture of *T. elongata* and RX**

**(A)** Cytogram showing the fluorescence of polyP-DAPI complexes (green fluorescence) and the fluorescence of DNA-SYTO®62 complexes (red fluorescence) in the mixed culture of *T. elongata* and RX prior to cell sorting.

**(B)** Proportion of polyP+ cells in the mixed culture of *T. elongata* and RX, labeled with DAPI prior to cell sorting and counted by flow cytometry (FCM) and epifluorescence microscopy (Epifluo).

**(C)** and **(D)** Cytograms showing the fluorescence of polyP-DAPI complexes (green fluorescence) and the fluorescence of DNA-SYTO®62 complexes (red fluorescence) in the **(C)** polyP+ and **(D)** polyP- fraction after cell sorting of the mixed culture of *T. elongata* and RX.

**(E)** and **(F)** Proportion of polyP+ cells in fractions **(C)** polyP+ and **(D)** polyP- after cell sorting of the mixed culture of *T. elongata* and RX and counted by flow cytometry (FCM) and epifluorescence microscopy (Epifluo).

Standard deviations are not shown for FCM because only one sample was counted per fraction.

**Figure 5: Comparison of JC-D7 and DAPI labeling for PAB detection**

Proportion of polyP+ cells, after PAB labeling with DAPI and SYTO®62 or with JC-D7 and SYTO®62. Cells were counted by flow cytometry (FCM) or epifluorescence microscopy (Epifluo). Significance was determined using one-way ANOVA test and Tukey's post-hoc test for multiple comparisons, denoted as follows: $^{*}p < 0.05$, $^{**}p < 0.001$, $^{***}p < 0.0005$, and $^{****}p < 0.0001$.